Title

Histologically resolved small RNA maps in primary focal segmental glomerulosclerosis indicate progressive changes within glomerular and tubulointerstitial regions.

Journal

Kidney International, 101(4)

Authors

Williams, Anna

Jensen, David

Pan, Xiaoqing

et al.

Publication Date

2022-04-01

DOI

10.1016/j.kint.2021.12.030

Peer reviewed

HHS Public Access

Author manuscript

Kidney Int. Author manuscript; available in PMC 2023 April 01.

Published in final edited form as:

Kidney Int. 2022 April ; 101(4): 766–778. doi:10.1016/j.kint.2021.12.030.

Histologically resolved small RNA maps in primary focal segmental glomerulosclerosis indicate progressive changes within glomerular and tubulointerstitial regions

Anna Marie Williams[1], **David M. Jensen**[1], **Xiaoqing Pan**[1,5], **Pengyuan Liu**[1], **Jing Liu**[1], **Sean Huls**[1], **Kevin R. Regner**[2], **Kenneth A. Iczkowski**[3], **Feng Wang**[1], **Junhui Li**[1], **Alexander J. Gallan**[3], **Tao Wang**[4], **Maria Angeles Baker**[1], **Yong Liu**[1], **Nava Lalehzari**[1], **Mingyu Liang**[1,#]

[1]Center of Systems Molecular Medicine, Department of Physiology, Medical College of Wisconsin, Milwaukee, WI 53226, USA

[2]Division of Nephrology, Department of Medicine, Medical College of Wisconsin, Milwaukee, WI 53226, USA

[3]Department of Pathology, Medical College of Wisconsin, Milwaukee, WI 53226, USA

[4]Division of Biostatistics, Institute of Health and Equity, Medical College of Wisconsin, Milwaukee, WI 53226, USA

[5]Department of Mathematics, Shanghai Normal University, Shanghai, China

Abstract

Pathological heterogeneity is common in clinical tissue specimens and complicates the interpretation of molecular data obtained from the specimen. As a typical example, a kidney biopsy specimen often contains glomeruli and tubulointerstitial regions with different levels of histological injury, including some that are histologically normal. We reasoned that the molecular profiles of kidney tissue regions with specific histological injury scores could provide new insights into kidney injury progression. Therefore, we developed a strategy to perform small RNA deep sequencing analysis for individually scored glomerular and tubulointerstitial regions in formalin-fixed, paraffin-embedded kidney needle biopsies. This approach was applied to study focal segmental glomerulosclerosis (FSGS), the leading cause of nephrotic syndrome in adults. Large numbers of small RNAs, including microRNAs, 3’ tRNA fragments (tRFs), 5’-tRFs, and mitochondrial tRFs, were differentially expressed between histologically indistinguishable

[#]Correspondence: Mingyu Liang, MB, PhD, Center of Systems Molecular Medicine, Department of Physiology, Medical College of Wisconsin, 8701 Watertown Plank Road, Milwaukee, WI 53226, Tel: 414-955-8539, FAX: 414-955-6546, mliang@mcw.edu.

Author Contributions

The project was conceived by ML and designed by AMW, MAB, and ML. AMW, DMJ, JL, SH, YL, and NL performed experiments. XP and PL analyzed the sequencing data. KRR, KAI, FW, JL, and AJG performed pathological analysis. AMW, DMJ, XP, PL, TW, and ML performed statistical analysis. AMW, DMJ, XP, JL, and ML drafted the manuscript. All authors edited or approved the manuscript.

Competing Interests

The authors declare no competing interests.

tissue regions from patients with FSGS and matched healthy controls. A majority of tRFs were upregulated in FSGS. Several small RNAs were differentially expressed between tissue regions with different histological scores in FSGS. Notably, with increasing levels of histological damage, miR-21–5p was upregulated progressively and miR-192–5p was downregulated progressively in glomerular and tubulointerstitial regions, respectively. This study marks the first genome scale molecular profiling conducted in histologically characterized glomerular and tubulointerstitial regions. Thus, substantial molecular changes in histologically normal kidney regions in FSGS might contribute to initiating tissue injury or represent compensatory mechanisms. In addition, several small RNAs might contribute to subsequent progression of glomerular and tubulointerstitial injury, and histologically mapping small RNA profiles may be applied to analyze tissue specimens in any disease.

Graphical Abstract

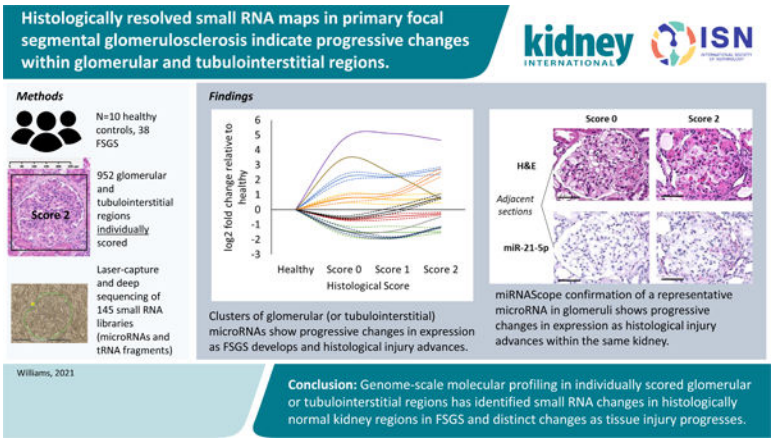

Keywords

Kidney; omics; microRNA; tRNA fragment; pathology

Introduction

Performing genome-scale molecular analysis in patient tissue specimens is a powerful approach for discovering potential molecular mechanisms underlying disease development. In addition, genome-scale molecular profiles in disease-relevant tissues provide a quantitative readout of the cumulative effect of all genetic and environmental factors and hold great promise for informing the precision medicine of multifactorial diseases [1, 2]. However, a major challenge for such analysis is the pathological heterogeneity that is prevalent in clinical tissue specimens. A tissue specimen obtained through biopsy or surgery will likely contain tissue regions at different stages of injury progression. Molecular analysis of the entire specimen or even a specific tissue type in the specimen will generate a molecular profile that is a summation of tissue regions at various stages of injury progression. Molecular changes that occur as a tissue type progresses from normal to injured within a patient, which could be mechanistically highly informative, may not be detected. Spatial transcriptomics and single-cell or single-nucleus omics analyses provide

great insights into spatial and cell type composition, but it remain challenging to resolve pathological heterogeneity using these approaches.

A typical example of this challenge is the analysis of kidney needle biopsy specimens. A biopsy specimen from a patient with kidney disease often contains glomeruli and tubulointerstitial (TI) regions with different levels of histological injury, including some that are histologically normal. Such pathological heterogeneity is common in kidney diseases and exemplified by focal segmental glomerulosclerosis (FSGS). FSGS is a leading cause of end-stage renal disease [3, 4]. The pathophysiological mechanism of primary FSGS is poorly understood. In a 3-dimensional, serial analysis of 104 tissue sections from 14 patients with primary FSGS, 72% of the 182 glomeruli assessed had various degrees of sclerosis, while 28% of glomeruli were histologically normal [5].

We reasoned that the molecular profiles of kidney tissue regions with specific histological injury scores could be highly informative about the regulatory networks involved in renal injury progression. Kidney biopsy specimens broadly available in pathological archives are usually formalin-fixed and paraffin-embedded (FFPE). Small RNA deep sequencing techniques, unlike genome-scale techniques for analyzing long RNA, proteins, or chromatin features, have unique feasibility in FFPE tissues [6]. We recently performed small RNA deep sequencing analysis in glomeruli and proximal tubules laser-captured from FFPE kidney biopsy specimens and identified tissue type-specific microRNA expression patterns associated with several kidney diseases [7]. MicroRNAs target specific messenger RNAs for degradation or translational repression and are well-established regulators of renal function and disease [8, 9]. Building on this experience, we developed a strategy in the present study to perform small RNA deep sequencing analysis for individually scored glomerular and surrounding TI regions in FFPE kidney needle biopsy specimens (Figure 1). We applied this strategy to study primary FSGS.

We analyzed tRNA fragments (tRFs) in addition to microRNAs. 3’- and 5’-tRFs may be produced through cleavage by Dicer of the T-loop and D-loop of tRNA, respectively. tRFs may have broad regulatory function, but the mechanisms are not well-understood [10–12]. Some 3’-tRFs may negatively regulate target mRNA abundance, similar to microRNAs [13, 14]. The involvement of tRFs in kidney disease is largely unknown [15].

Methods

Patients and kidney specimens

The study was approved by the Froedtert Health Office of Clinical Research and Innovative Care Compliance and the Institutional Review Board of the Medical College of Wisconsin (IRB 10841 and 21975). FFPE kidney needle biopsies originally collected between 1995–2013 were acquired from Froedtert Hospital pathological archives in Milwaukee, Wisconsin. Adult FSGS subjects were included if they were diagnosed with primary FSGS by a board-certified pathologist or nephrologist. Subjects were excluded with diagnosis or suspicion of secondary FSGS, the collapsing variant if noted in the original pathological report, dialysis at the time of biopsy, or other kidney pathological diagnoses such as acute kidney injury (AKI) or diabetic nephropathy. Adult healthy controls were trauma

subjects who had undergone nephrectomy due to gunshot wound, stab wound, or motor vehicle accident. Subjects were excluded for hypertension, diabetes, serum creatinine (SCr) ≥ 1.2 mg/dl, blood pressure < 90/60, incidental findings on the pathology report such as glomerulosclerosis or interstitial fibrosis, or previous record of kidney injury such as AKI or chronic kidney disease (CKD). Nephrectomy tissue sections were selected from the unaffected kidney parenchyma to minimize the number of red blood cells present. Hematoxylin and Eosin (H&E) stained slides were examined by 2 board-certified pathologists to assess the biopsy for pathological abnormalities and trauma-related injury such as necrosis. Matching between FSGS subjects and healthy controls was assessed using a Mann-Whitney Rank Sum test for age, and a Fischer's exact test for gender and race. The following clinical values were collected from the time of biopsy or nephrectomy: age, gender, race, systolic blood pressure (SBP), diastolic blood pressure (DBP), SCr, blood urea nitrogen (BUN), and estimated glomerular filtration rate (eGFR).

Reference standards for assessing library and sequencing quality

To assess library and sequencing quality, we generated 3 reference standards. A fresh glomeruli reference standard was generated from hundreds of glomeruli isolated from fresh nephrectomy samples obtained from 10 subjects using cold sieving followed by manual selection as we described [16]. The fresh tissue used was normal tissue adjacent to cancer tissue with some subjects having diabetes, hypertension, or glomerulosclerosis. One aliquot of the fresh glomeruli reference standard was run in parallel with experimental samples for each run of library preparation to assess batch to batch reproducibility of library preparation and sequencing. The data quality was considered acceptable if the Pearson's correlation of log-transformed read counts was > 0.985 between technical replicates of the reference standard in different runs. An FFPE glomerular reference standard and an FFPE TI reference standard were also generated from approximately 600 regions from tissue specimens from 10 healthy controls, using subjects independent from the healthy controls used for experimental comparison. Matching between healthy controls used for experimental samples and healthy controls used for FFPE reference standards was assessed using a Mann-Whitney Rank Sum test for age, and a Fischer's exact test for gender and race. Each FFPE reference standard was sequenced in technical triplicate, and individual experimental glomerular and TI region microRNA libraries were compared to the respective FFPE reference standard samples using Pearson's correlation of log-transformed read counts.

Tissue sectioning

The approach for mapping small RNA profiles to specific histological scores in specific tissue types was summarized in Figure 1. Three serial 5μm thick slices were cut. The first slice was mounted on a slide, stained with H&E, and scanned into NanoZoomer software. The second and third 5μm thick slices from the FFPE tissue block were mounted onto the specialized membrane slide which was pre-treated with UV light used for laser capture microdissection (LCM).

Histological scoring

Semiquantitative scoring methods were adapted from previously described scoring methods [5]: score 0 – 0%, score 1 – 1–25%, score 2 – 26–50%, and score 3 – >50%; glomerular

regions were scored based on percentage of sclerosis, and TI regions were scored for fibrosis, cell infiltration, and/or tubular atrophy. Each glomerular region was labelled with a letter in Nanozoomer Software. The glomerular and TI regions for FSGS patients and healthy controls were scored by a blinded board-certified pathologist and a blinded board-certified nephrologist. Any differences in scoring was assessed by a third blinded pathologist. Histological scoring of TI regions was conducted following LCM in order to accurately draw the region borders in Nanozoomer Software. Glomerular or TI regions with score 3 were not utilized due to the small number of cells remaining in those regions.

Laser capture microdissection (LCM)

LCM was conducted by methods previously described [7] using a Zeiss P.A.L.M. Microbeam III LCM system (Carl Zeiss Microscopy). Each individual region was visually identified and labelled with its corresponding letter using the H&E images in Nanozoomer Software. First, the glomerular region was collected; then, to collect the surrounding TI region, a square containing approximately the same tissue volume as the glomerular region was captured. Approximately 150,000–1,000,000 μm^3 total sample volume was collected for each individual glomerular or TI region.

Total RNA extraction

Total RNA was extracted from FFPE samples using a Qiagen AllPrep RNA/DNA FFPE kit and from the fresh glomeruli reference standard using a Qiagen AllPrep DNA/RNA Mini Kit according to the manufacturer's protocol for extraction of small RNAs. For FSGS samples, up to 3 regions per score per subject were pooled for RNA extraction. If more than 3 regions were present on a biopsy for a given score, regions were prioritized based on largest total sample volume and agreement in scoring between the 2 blinded health professionals. Only TI regions associated with experimental glomerular regions were used in analysis. For healthy controls, 3 histological normal glomerular or TI regions were pooled per subject. The fresh glomeruli reference standard contained several hundred fresh glomeruli and the FFPE reference standards contained around 600 FFPE tissue regions, as indicated above. RNA was eluted in 20 and 500 μl of DEPC water for the FFPE samples and the fresh glomeruli reference standard, respectively.

Small RNA deep sequencing

An Illumina TruSeq Small RNA Library Kit was used to prepare small RNA deep sequencing libraries as described with modifications [7]. Each batch of library preparation included a fresh glomeruli reference standard aliquot to assess batch to batch consistency of library preparation and sequencing. cDNA was amplified from experimental samples with 21 cycles of PCR, and reference standards with 15 cycles of PCR. The size distribution of cDNA generated for each library was assessed using a DNA 1000 chip on an Agilent 2000 Bioanalyzer. Forty-eight samples were multiplexed per lane and sequenced with 2x125 bp reads on a Hi-Seq 2500 sequencer.

Analysis of Small RNA Deep Sequencing Data

The process of small RNA deep sequencing data analysis was depicted in Supplemental Figure S1 [18–21]. Adaptor sequences were removed from raw data using cutadapt. FASTQC was used to trim sequences with base quality < 13 and to remove reads > 30 or < 15 base pairs. Transcripts were mapped to the human genome utilizing the human hg38 USCS genome annotation using BWA. MicroRNAs were mapped to the Small RNA annotation using BEDtools. tRFs were mapped to GtRNAdb using BWA. Small RNA libraries with > 300,000 mapped reads and > 0.70 average correlation of microRNAs with the FFPE reference standard technical triplicates were included in the study. Small RNAs detectable in ≥ 50% of samples in at least one of the two groups in each comparison were included in analysis. Using DESeq2, differential expression of microRNAs and tRFs was assessed for glomerular and TI regions between scores 0, 1, and 2, and healthy controls. The Benjamini-Hochberg method was used to control false discovery rate (FDR); FDR < 0.05 was considered statistically significant. Log_2 Fold Change was calculated and graphed for significantly differentially expressed small RNAs.

miRNAScope Analysis

MicroRNA in situ hybridization analysis was performed using miRNAScope HD reagent kit-Red from ACD (Cat. No. 324500) following the manufacturer's instructions. Kidney sections (4 μm) were baked for 1 h at 60°C, de-paraffinized with xylene and 100% ethanol, and incubated with 12% formaldehyde for 2 h at room temperature (RT) for post-fixation. Sections were pretreated with hydrogen peroxide for 10 min at RT followed by target retrieval for 15 min at 100°C and protease treatment for 30 min at 40°C. Probes (Scramble, Ref: 727881-S1; RNU6, Ref: 727871-S1; hsa-miR-21–5p, Ref: 728561-S1) were then hybridized for 2 h at 40°C followed by miRNAScope amplification and chromogenic detection. Sections were counterstained by 50% hematoxylin, cleared in xylene, and mounted with EcoMount.

Target Gene Analysis

Genes with "strong evidence" for being targeted by a microRNA were obtained from miRTarBase [22]. miRTarBase defines "strong evidence" as experimental evidence from reporter assay, western blot, or qPCR data. Target genes for 3'-tRFs were predicted using miRDB because 3'-tRFs may act through microRNA-like mechanisms. No established methods were available for predicting target genes for 5'-tRFs. Pathway analysis for predicted or experimentally supported target genes was conducted using Metascape Pathway Analysis, which reports pathways or biological terms from databases such as Kyoto Encyclopedia of Genes and Genomes (KEGG) and Gene Ontology. Statistically significantly enriched pathways or biological terms were hierarchically clustered into a tree based on Kappa-statistical similarities among their gene memberships. One term from each cluster is selected to represent the cluster.

Real-Time quantitative PCR

A select microRNA was measured using TaqMan microRNA assays following the manufacturer's protocol [23]. mRNA was measured using SYBR Green real-time quantitative

PCR (qPCR). cDNA was synthesized using the RevertAid First-Strand cDNA Synthesis Kit (ThermoFisher), and qPCR was performed using Bullseye EvaGreen qPCR Master Mix (MedSci). Technical triplicates were run for each experimental sample on an Applied Biosystems real-time PCR instrument. 5S rRNA and 18S rRNA was used to normalize expression levels of microRNA and mRNA, respectively. The absence of genomic DNA interference was verified using negative control reactions that did not contain reverse transcription reagents. Statistical significance was assessed using ANOVA; $p < 0.05$ was considered statistically significant.

Results

Patient characteristics and histological scores of individual glomerular and TI regions

Thirty-eight FSGS subjects and 10 healthy controls were included in the study (Table 1). There were no significant differences between FSGS subjects and healthy controls for age (p=0.82), gender (p=0.72), or race (p=0.35). The healthy controls and FSGS subjects were 20% and 18% female, and 50% and 55% African American, respectively. SCr and BUN were higher and eGFR was lower in FSGS patients compared to healthy controls. Pathological classification of FSGS variants was not available in the original pathological reports for most patients. A re-analysis of slides used in the original pathological diagnosis by a board-certified pathologist indicated the presence of not otherwise specified, collapsing, and perihilar variants in our cohort at expected frequencies (Supplemental Table S1). APOL1 genotype information was not available for these patients. Attempts were made to perform APOL1 genotyping using DNA extracted from FFPE kidney biopsy specimens but were not successful likely because the DNA was highly fragmented.

Supplemental Figure S2 shows representative images of glomerular and TI regions with score 0, 1, 2 or 3. Glomerular regions were scored based on percentage of sclerosis, and TI regions were scored for fibrosis, cell infiltration, and/or tubular atrophy. A summary of the histological score distribution for each subject is listed in Supplemental Table S1. A total of 476 glomerular and 476 TI regions were scored: for glomerular regions, 173 score 0, 58 score 1, 63 score 2, and 182 score 3; for TI regions, 88 score 0, 86 score 1, 105 score 2, and 197 score 3. The number of glomeruli available on the sections cut for the current study may not be the same as that on the original diagnostic sections. Representative images of the serial cuts for H&E staining and LCM are shown in Supplemental Figure S3.

Quality of small RNA deep sequencing

Age, gender and race composition of healthy control subjects used for constructing FFPE reference standards did not differ significantly from those of the FSGS patients or healthy controls used for experimental groups (Supplementary Table S2).

For all 15 fresh glomeruli reference standard aliquots sequenced, the correlations of log-transformed microRNA abundance among individual sequencing runs ranged from 0.987–0.998. MicroRNA profiles of fresh and FFPE glomerular reference standards were also highly correlated. MicroRNA profiles of most experimental glomerular and TI regions correlated well with FFPE glomerular and TI reference standards, respectively. Examples of

these correlations are shown in Supplementary Figure S4. As expected, the correlations between glomerular and TI microRNA profiles were lower compared to correlations between samples of the same tissue type.

Seventeen small RNA libraries were excluded because they had < 300,000 mapped reads or showed < 0.70 correlation of microRNA profiles with the FFPE reference standards. A total of 145 small RNA libraries were included in the subsequent analysis, 78 samples from glomerular regions and 67 samples from TI regions. A summary of the 145 samples, including tissue type, histological score, total sequencing reads, mapping rate, and other quality indexes, is shown in Supplementary Table S3. On average, each library contained 2,475,893 mapped reads and had a 58.9% mapping rate. Demographic and clinical information for healthy control subjects and FSGS patients who were included in the 78 glomerular samples and 67 TI samples that fulfilled the quality control standards are shown in Supplemental Table S4 and S5. A total of 160 microRNAs, 229 3’ tRFs, and 94 5’ tRFs were detected in FSGS and healthy control samples.

Differentially expressed microRNAs

In glomerular regions, 29 microRNAs were differentially expressed between FSGS score 0 (i.e., histologically normal glomeruli in FSGS patients) compared to normal glomeruli from healthy control subjects (Figure 2A). Within FSGS patients, 11 differentially expressed microRNAs were identified between score 2 and score 0 (Figure 2B), and 7 differentially expressed microRNAs between score 1 and score 2 (Figure 2C). No significantly differentially expressed microRNAs were detected between score 1 and score 0.

Glomerular microRNAs that were differentially expressed in at least one of these comparisons exhibited several distinct patterns of expression changes as glomeruli progress from healthy controls to increasing histological scores in FSGS patients (Figure 2D, 2E). For example, the expression of miRs-12136, −145–5p, and −15b-5p progressively increased stepwise as histological score increased. miRs-204–5p, −21–3p, and −21–5p showed an initial decrease in score 0 compared to healthy controls, but progressively increased across score 1 and score 2 in glomeruli. Other groups remained consistently increased or decreased across histological scores compared to healthy controls.

In TI regions, 26 microRNAs were differentially expressed between FSGS score 0 (i.e., histologically normal TI regions in FSGS patients) compared to normal TI regions from healthy control subjects (Figure 3A). Within FSGS patients, 1 microRNA was identified as differentially expressed between score 1 and score 0 (Figure 3B), 5 between score 2 and score 0 (Figure 3C), and 3 between score 2 and score 1 (Figure 3D).

TI microRNAs could also be divided into several groups based on their patterns of progressive expression changes, but the specific patterns for several microRNAs were different between TI and glomerular microRNAs (Figure 3E, 3F). For example, miR-378a-3p, −204–5p, −10b-5p, −192–5p, and −12136 decreased progressively from healthy controls to scores 0, 1, and 2 in FSGS. miR-194–5p initially increased in score 0 TI samples, but decreased across histological scores with score 2 showing less expression compared to heathy controls. Similar to glomerular microRNAs, several groups of TI

microRNAs remained relatively constant across increasing histological scores but were nonetheless differentially expressed compared to healthy controls.

Several notable microRNAs with known roles in the kidney were found to be differentially expressed between histological scores. miR-21–5p was significantly increased in score 2 glomeruli compared to both score 0 and score 1 glomeruli (Figure 4A). miR-146b-5p was significantly increased in score 2 glomeruli compared to score 0 glomeruli. Score 0 samples showed significantly higher expression of miR-146b-5p than healthy control glomeruli (Figure 4B). miR-192–5p was significantly decreased in score 2 TI samples compared to both score 0 and score 1 TI samples (Figure 4C). Additionally, a novel microRNA with no reported function in nephropathy, miR-12136, was found to be significantly lower in score 2 TI samples compared to both score 0 and score 1 TI samples (Figure 4D). In situ hybridization using the miRNAScope method was performed for miR-21–5p on additional sections from two patients. miR-21–5p signals detected in individual glomeruli were mapped to histological injury scores obtained from adjacent, H&E sections. The analysis confirmed upregulation of miR-21–5p in score 2 glomeruli compared with score 0 glomeruli in the same biopsy specimen (Figure 4E).

Differentially expressed tRFs

In glomerular regions, 11 3’-tRFs (1 mitochondrial, 10 cytosolic) and 27 5’-tRFs (1 mitochondrial, 26 cytosolic) were differentially expressed between FSGS score 0 compared to healthy controls (Figure 5A and C). Additionally, 1 differentially expressed cytosolic 3’-tRF was identified between score 2 and score 1 in FSGS (Figure 5B). Most (81%) of these tRFs were increased in score 0 compared to healthy controls and remained increased through scores 1 and 2 (Figure 5D, 5E). A small number of tRFs were decreased in score 0 compared to healthy controls and remained decreased as histological injury progressed. M3-tRNA-iMet-CAT-1–8_21 appeared to fluctuate as glomeruli progressed from healthy control to various histological scores in FSGS, although only the change from score 0 to 1 reached statistical significance.

In TI regions, 32 3’-tRFs (8 mitochondrial, 24 cytosolic) and 24 5’-tRFs (2 mitochondrial, 22 cytosolic) were differentially expressed between TI score 0 and healthy controls (Figure 6A and C). Additionally, 1 differentially expressed cytosolic 3’-tRF was identified between score 2 and score 0 in FSGS (Figure 6B). Similar to glomerular tRFs, most (83%) of the differentially expressed tRFs in TI regions, especially 3’-tRFs, were increased in score 0 compared to healthy controls and remained increased through scores 1 and 2 (Figure 6D, 6E).

Target gene and pathway analysis

The 29 microRNAs differentially expressed in glomeruli between healthy controls and score 0 in FSGS have been experimentally shown to target 574 genes based on miRTarBase. The 12 microRNAs differentially expressed in glomeruli from FSGS patients between scores 0, 1 and 2 have 539 experimentally supported target genes. microRNAs differentially expressed between scores 0, 1 and 2 were combined for the target gene analysis because the number of differentially expressed microRNAs in each of these comparisons was small. Several

pathways or Gene Ontology terms were over-represented in target genes of microRNAs differentially expressed between healthy control vs. score 0 as well as between scores 0, 1, and 2 (Figure 7A). However, some pathways were over-represented in only one of the two groups. For example, Gene Ontology terms “blood vessel development” and “response to oxygen levels” were enriched in target genes of microRNAs differentially expressed between scores 0, 1, and 2 but not between healthy control and score 0.

The 26 microRNAs differentially expressed in TI regions between healthy controls and score 0 in FSGS have 801 experimentally supported target genes. The 5 microRNAs differentially expressed in TI regions from FSGS patients between scores 0, 1, and 2 have 121 experimentally supported target genes. Again, several pathways or biological terms were over-represented in only one of the two groups of genes (Figure 7B).

For 11 and 32 3’-tRFs that were differentially expressed in glomeruli and TI regions, respectively, between healthy controls and FSGS score 0, and were at least 17 nucleotides long, 1,668 and 5,336 unique genes were predicted by miRDB as potential target genes. These predicted target genes were enriched for several pathways and Gene Ontology terms (Supplemental Figure S5). Target gene analysis was not performed for 5’-tRFs because methods for predicting 5’-tRF target genes were not available or for 3’-tRFs differentially expressed between scores in FSGS because only one was identified in each tissue type.

Validation of a select microRNA and target gene

miR-146–5p was up-regulated in score 0 glomeruli from FSGS patients compared to normal glomeruli from healthy controls and further up-regulated in score 2 glomeruli in FSGS (Figure 4B). Tumor necrosis factor receptor-associated factor 6 (TRAF6) is a direct target of miR-146b-5p through which miR-146b-5p may exert negative feedback on pro-fibrotic and pro-inflammatory NFκB (nuclear factor kappa-light-chain-enhancer of activated B cells) signaling (Figure 8A) [24]. We confirmed the upregulation of miR-146b-5p in score 2 glomeruli compared to healthy controls and score 0 glomeruli by performing qPCR analysis on the original RNA samples (Figure 8B). The upregulation in score 0 compared to healthy controls approached significance (p=0.14). Conversely, TRAF6 was downregulated in score 2 glomeruli compared to score 0 and healthy controls (Figure 8C).

Discussion

For the first time, genome-scale molecular profiling was conducted in histologically characterized individual glomerular or TI regions. To accomplish this, we developed an approach that combines the scoring of individual glomerular and TI regions and laser-capture microdissection of these regions in adjacent sections, followed by small RNA deep sequencing analysis. We applied this approach to analyze FFPE kidney tissues from healthy controls and FSGS patients and obtained a wealth of previously unavailable molecular profiles associated with glomeruli and TI regions with specific histological scores.

The study revealed broad differences in small RNA expression profiles between glomeruli and TI regions in healthy control subjects and histologically normal glomeruli and TI regions in FSGS patients. These glomeruli and TI regions are histologically

indistinguishable between the two groups of subjects. These findings indicate that glomeruli and TI regions in FSGS patients are undergoing substantial molecular changes before there is any overt histological injury. The molecular changes may result from systemic factors that cause the development of FSGS or other systemic changes or medications associated with FSGS [3, 4]. These early molecular changes may contribute to initiating the development of histological injuries that are the hallmark of FSGS or represent compensatory mechanisms that keep some tissue regions normal at this stage of FSGS development. As histological injury advances in FSGS, additional changes in small RNA expression occur in glomeruli and TI regions, which may contribute to driving the progression of histological injury and, ultimately, the progression of CKD.

This study provides an unprecedented level of tissue type and histological score resolution for the expression pattern of several microRNAs with prominent functional roles in the kidney. For example, miR-21–5p contributes the progression of chronic renal injury [25–27]. We found miR-21–5p was significantly upregulated in glomerular regions with score 2 versus score 0 and with score 2 versus score 1 in FSGS. miR-146b-5p is upregulated in kidneys from patients with FSGS or membranoproliferative glomerulonephritis [7]. In a rat model of CKD, miR-146b knockout exacerbated kidney injury in female, but not male, rats [28]. We found that miR-146b-5p was more highly expressed in score 2 glomeruli compared to score 0 glomeruli in FSGS. In addition, miR-146b-5p target gene TRAF6 was down-regulated as glomerular injury progressed. We suspect that the upregulation of miR-146b-5p and downregulation of proinflammatory TRAF5 in more severely injured samples might be a compensatory response to increased inflammation and injury. miR-192–5p is highly abundant in the kidney and downregulated in human kidneys with hypertension or hypertensive nephrosclerosis, and rodent studies have shown that renal miR-192 is protective against the development of hypertension by targeting ATP1B1 (β1 subunit of Na^+/K^+-ATPase) [16, 20, 29, 30]. miR-192–5p was significantly downregulated in TI regions with score 2 versus score 0 and with score 2 versus score 1 in FSGS. This study also identified substantial, progressive changes for microRNAs that have not been previously reported as relevant to kidney disease; an example is miR-12136.

Another novel aspect of this study was the investigation of tRFs, which have not been studied in depth in kidney disease [15]. The human genome encodes 49 different cytosolic tRNAs and 22 mitochondrial tRNAs. tRFs are 14–30 nucleotide fragments of tRNAs produced through enzymatic cleavage [10, 11]. Using similar mechanisms to microRNAs, some 3’-tRFs decrease the abundance of sequence-complementary mRNAs and proteins in a cell type-specific manner [13, 14, 31], whereas 5’-tRFs can reduce global translation rates by 10–15% [32]. In this study, we found substantial differences in tRFs between healthy controls and histologically normal tissue regions from FSGS, most of which were up-regulated in FSGS. The finding is consistent with reported upregulation of tRF generation during early stages of stress [12, 33]. In addition, the finding further demonstrates that substantial molecular changes in glomeruli and TI regions precede overt histological injury in FSGS.

This study had several limitations. First, in a comparison between any two FSGS scores, some, but not all, subjects were represented in both groups. We attempted to apply a linear mixed model to account for the subject overlap, but the model was not stable, and the

statistics did not converge. This was likely due to the large number of subjects having samples with score 0 and score 1 in glomerulus regions, and score 1 and score 2 in TI regions, but only a small number of subjects having all 3 scores. Therefore, we treated each score as individual groups in the statistical analysis, without consideration of the subject overlap. Second, FSGS includes several pathological variants [34]. We did not analyze each of the variants separately, which would likely require a larger sample size. Third, proteinuria values were not collected for FSGS subjects because methods of measurement varied between patients ranging from protein dipstick to 24-hour urinary analysis. Fourth, it is possible that some of the expression changes detected may be due to changes in the heterogeneous composition of the cell population present in the samples as histological injury progresses. Fifth, it remains to be determined whether the changes in microRNAs and tRFs that we observed are specific to FSGS. In the previous study of four types of kidney disease (without separation of histological injury scores), we identified some microRNAs in glomeruli that were differentially expressed between different kidney diseases, but none in proximal tubules [7]. Lastly, the library preparation techniques used in this study only detect tRFs cleaved by Dicer due to specialized universal adaptors in the Illumina TruSeq Small RNA Library Kit. 3’-tRFs can also be produced by angiogenin and nucleases from the ribonuclease A superfamily [10, 14, 17, 35].

The approach that we developed for histologically mapping small RNA profiles may be applied to analyze tissue specimens in any disease. We chose primary FSGS for this study for several reasons. FSGS patients are likely to have multiple glomeruli and TI regions with highly variable histological scores in a needle biopsy specimen because of the focal nature of FSGS pathology. While secondary FSGS has a known cause such as hypertension and human immunodeficiency virus infection, primary FSGS has an unknown etiology, lacks animal and cell models, and has limited treatment options [3, 4]. However, our approach for histologically mapping small RNA profiles may be applied to study other kidney pathologies and diseases as well as non-kidney diseases. The approach is particularly powerful as it can be used to analyze FFPE specimens, which are available in large numbers in pathological archives.

Supplementary Material

Refer to Web version on PubMed Central for supplementary material.

Funding

This work was supported by the Advancing a Healthier Wisconsin Endowment and the National Institutes of Health (HL121233, HL149620, DK098104). J. Liu was supported by T32 HL134643 and the Cardiovascular Center’s A.O. Smith Fellowship Scholars Program.

Data Availability

Raw read count data from the deep sequencing analysis are provided as supplemental datasets.

References

1. Kotchen TA, Cowley AW Jr., and Liang M, Ushering Hypertension Into a New Era of Precision Medicine. JAMA, 2016. 315(4): p. 343–4. [PubMed: 26769233]
2. Mattson DL and Liang M, Hypertension: From GWAS to functional genomics-based precision medicine. Nat Rev Nephrol, 2017. 13(4): p. 195–196. [PubMed: 28262776]
3. D'Agati VD, Kaskel FJ, and Falk RJ, Focal segmental glomerulosclerosis. N Engl J Med, 2011. 365(25): p. 2398–411. [PubMed: 22187987]
4. Fogo AB, Causes and pathogenesis of focal segmental glomerulosclerosis. Nat Rev Nephrol, 2015. 11(2): p. 76–87. [PubMed: 25447132]
5. Fuiano G, et al. , Serial morphometric analysis of sclerotic lesions in primary "focal" segmental glomerulosclerosis. J Am Soc Nephrol, 1996. 7(1): p. 49–55. [PubMed: 8808109]
6. Buitrago DH, et al. , Small RNA sequencing for profiling microRNAs in long-term preserved formalin-fixed and paraffin-embedded non-small cell lung cancer tumor specimens. PLoS One, 2015. 10(3): p. e0121521. [PubMed: 25812157]
7. Baker MA, et al. , Tissue-Specific MicroRNA Expression Patterns in Four Types of Kidney Disease. J Am Soc Nephrol, 2017. 28(10): p. 2985–2992. [PubMed: 28663230]
8. Liang M, et al. , MicroRNA: a new frontier in kidney and blood pressure research. Am J Physiol Renal Physiol, 2009. 297(3): p. F553–8. [PubMed: 19339633]
9. Trionfini P and Benigni A, MicroRNAs as Master Regulators of Glomerular Function in Health and Disease. J Am Soc Nephrol, 2017. 28(6): p. 1686–1696. [PubMed: 28232619]
10. Lee YS, et al. , A novel class of small RNAs: tRNA-derived RNA fragments (tRFs). Genes Dev, 2009. 23(22): p. 2639–49. [PubMed: 19933153]
11. Guzzi N, et al. , Pseudouridylation of tRNA-Derived Fragments Steers Translational Control in Stem Cells. Cell, 2018. 173(5): p. 1204–1216 e26. [PubMed: 29628141]
12. Magee R and Rigoutsos I, On the expanding roles of tRNA fragments in modulating cell behavior. Nucleic Acids Res, 2020. 48(17): p. 9433–9448. [PubMed: 32890397]
13. Maute RL, et al. , tRNA-derived microRNA modulates proliferation and the DNA damage response and is down-regulated in B cell lymphoma. Proc Natl Acad Sci U S A, 2013. 110(4): p. 1404–9. [PubMed: 23297232]
14. Li Z, et al. , Extensive terminal and asymmetric processing of small RNAs from rRNAs, snoRNAs, snRNAs, and tRNAs. Nucleic Acids Res, 2012. 40(14): p. 6787–99. [PubMed: 22492706]
15. Pan X, et al. , Transfer RNA Fragments in the Kidney in Hypertension. Hypertension, 2021. 77(5): p. 1627–1637. [PubMed: 33775129]
16. Mladinov D, et al. , MicroRNAs contribute to the maintenance of cell-type-specific physiological characteristics: miR-192 targets Na+/K+-ATPase beta1. Nucleic Acids Res, 2013. 41(2): p. 1273–83. [PubMed: 23221637]
17. Maraia RJ and Lamichhane TN, 3' processing of eukaryotic precursor tRNAs. Wiley Interdiscip Rev RNA, 2011. 2(3): p. 362–75. [PubMed: 21572561]
18. Kriegel AJ, et al. , Characteristics of microRNAs enriched in specific cell types and primary tissue types in solid organs. Physiol Genomics, 2013. 45(23): p. 1144–56. [PubMed: 24085797]
19. Widlansky ME, et al. , miR-29 contributes to normal endothelial function and can restore it in cardiometabolic disorders. EMBO Mol Med, 2018. 10(3).
20. Liu Y, et al. , MicroRNA-214–3p in the Kidney Contributes to the Development of Hypertension. J Am Soc Nephrol, 2018. 29(10): p. 2518–2528. [PubMed: 30049682]
21. Yao D, et al. , OncotRF: an online resource for exploration of tRNA-derived fragments in human cancers. RNA Biol, 2020. 17(8): p. 1081–1091. [PubMed: 32597311]
22. Huang HY, et al. , miRTarBase 2020: updates to the experimentally validated microRNA-target interaction database. Nucleic Acids Res, 2020. 48(D1): p. D148–D154. [PubMed: 31647101]
23. Kriegel AJ, et al. , Endogenous microRNAs in human microvascular endothelial cells regulate mRNAs encoded by hypertension-related genes. Hypertension, 2015. 66(4): p. 793–9. [PubMed: 26283043]

24. Taganov KD, et al. , NF-kappaB-dependent induction of microRNA miR-146, an inhibitor targeted to signaling proteins of innate immune responses. Proc Natl Acad Sci U S A, 2006. 103(33): p. 12481–6. [PubMed: 16885212]
25. Dey N, et al. , MicroRNA-21 orchestrates high glucose-induced signals to TOR complex 1, resulting in renal cell pathology in diabetes. J Biol Chem, 2011. 286(29): p. 25586–603. [PubMed: 21613227]
26. Chau BN, et al. , MicroRNA-21 promotes fibrosis of the kidney by silencing metabolic pathways. Sci Transl Med, 2012. 4(121): p. 121ra18.
27. Lai JY, et al. , MicroRNA-21 in glomerular injury. J Am Soc Nephrol, 2015. 26(4): p. 805–16. [PubMed: 25145934]
28. Paterson MR, Geurts AM, and Kriegel AJ, miR-146b-5p has a sex-specific role in renal and cardiac pathology in a rat model of chronic kidney disease. Kidney Int, 2019. 96(6): p. 1332–1345. [PubMed: 31668631]
29. Baker MA, et al. , MiR-192–5p in the Kidney Protects Against the Development of Hypertension. Hypertension, 2019. 73(2): p. 399–406. [PubMed: 30595117]
30. Tian Z, et al. , MicroRNA-target pairs in the rat kidney identified by microRNA microarray, proteomic, and bioinformatic analysis. Genome Res, 2008. 18(3): p. 404–11. [PubMed: 18230805]
31. Telonis AG, et al. , Dissecting tRNA-derived fragment complexities using personalized transcriptomes reveals novel fragment classes and unexpected dependencies. Oncotarget, 2015. 6(28): p. 24797–822. [PubMed: 26325506]
32. Yamasaki S, et al. , Angiogenin cleaves tRNA and promotes stress-induced translational repression. J Cell Biol, 2009. 185(1): p. 35–42. [PubMed: 19332886]
33. Fu H, et al. , Stress induces tRNA cleavage by angiogenin in mammalian cells. FEBS Lett, 2009. 583(2): p. 437–42. [PubMed: 19114040]
34. D'Agati VD, et al. , Pathologic classification of focal segmental glomerulosclerosis: a working proposal. Am J Kidney Dis, 2004. 43(2): p. 368–82. [PubMed: 14750104]
35. Kumar P, et al. , tRFdb: a database for transfer RNA fragments. Nucleic Acids Res, 2015. 43(Database issue): p. D141–5. [PubMed: 25392422]

Translational Statement

This study has mapped genome-wide changes in small RNA expression to specific, histologically scored glomerular and tubulointerstitial regions in FSGS patients. These histologically mapped small RNA changes may be explored as a new type of biomarkers for tissue injury or disease progression in patients or to drive mechanistic studies leading to new targeted therapeutics. The approach for histologically mapping small RNA profiles may be applied to analyze tissue specimens in any disease.

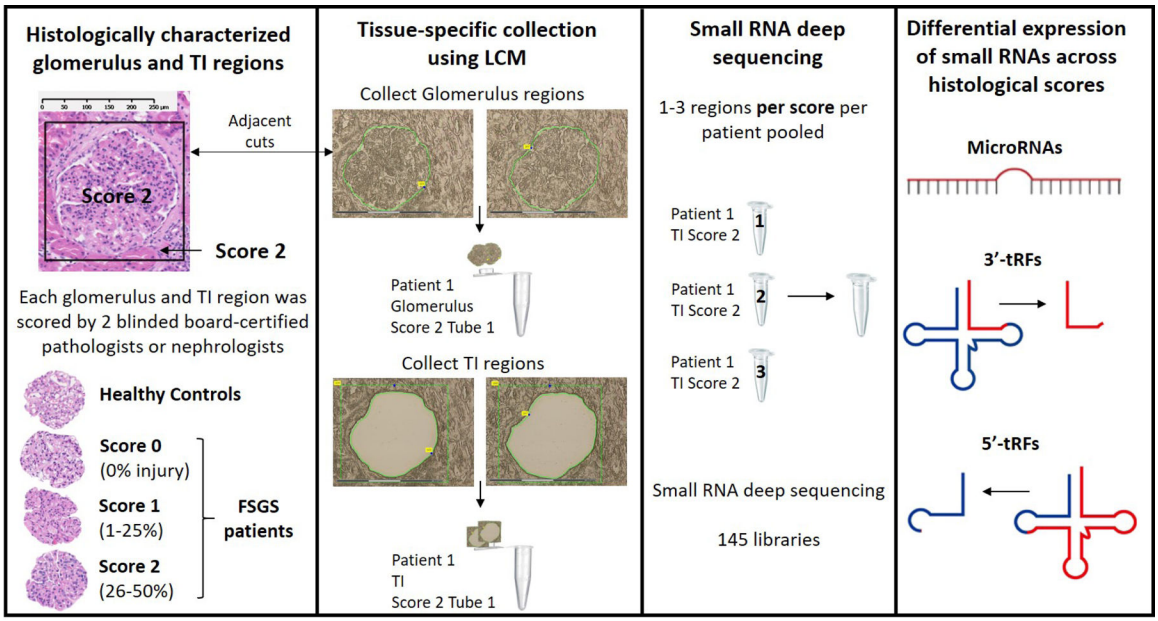

Figure 1. Approach for mapping small RNA profiles to specific histological scores in specific tissue types.

For each FFPE kidney tissue block from healthy control subjects or FSGS patients, 3 consecutive cuts were made. The first tissue section was H&E stained and each glomerular region and the surrounding tubulointerstitial (TI) region scored for histological injury by 2 blinded board-certified pathologists or nephrologists. Inconsistent scores were reviewed and scored by a third pathologist. The second and third cuts made from the FFPE tissue block were used for laser capture microdissection (LCM). First, the glomerular regions were cut, then the surrounding TI regions. Up to three regions per score per patient were pooled for small RNA library preparation and deep sequencing. Differential expression of microRNAs, 3'-tRFs, and 5'-tRFs was assessed across histological scores in glomerular and TI regions.

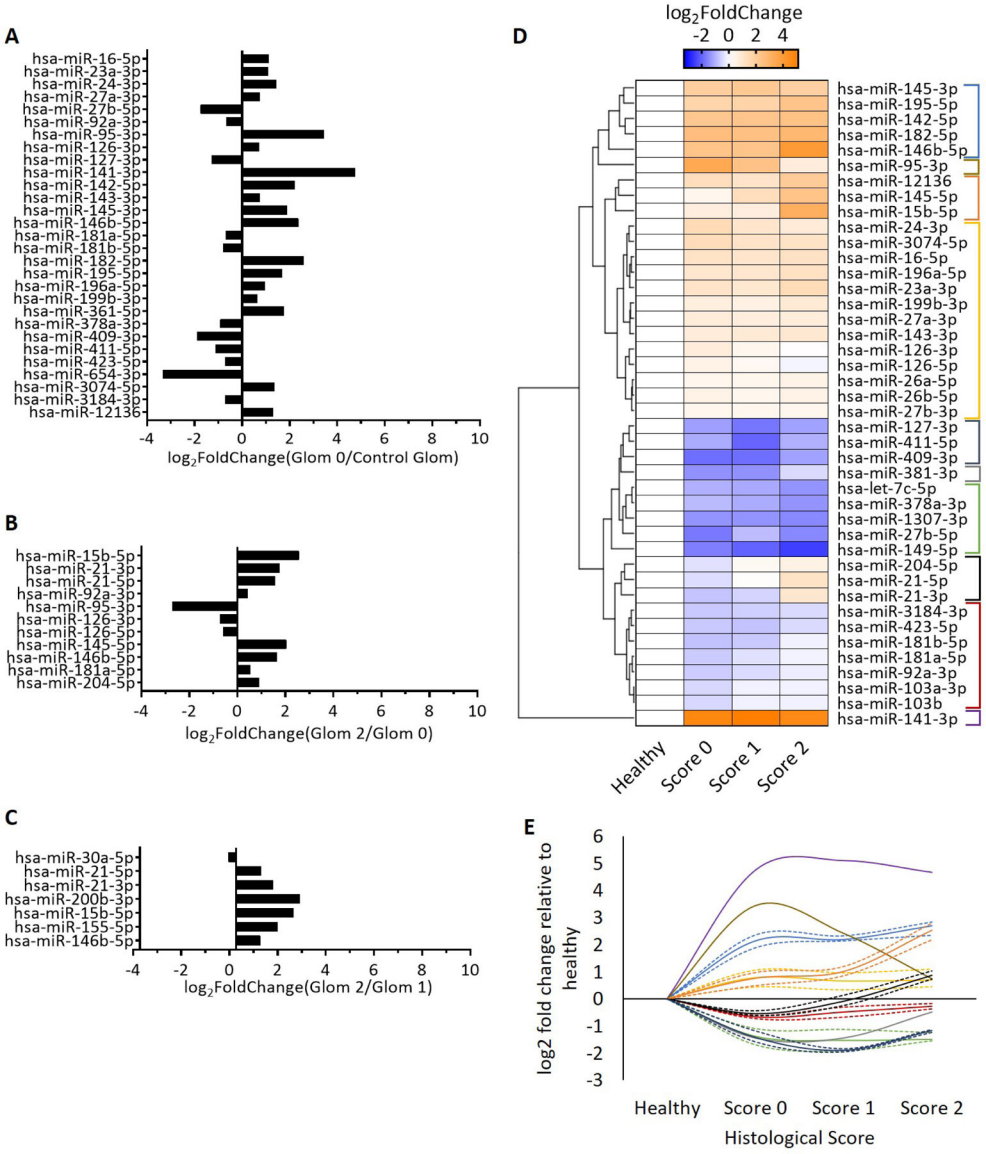

Figure 2. Glomerular microRNAs show progressive changes in expression as FSGS develops and histological injury advances.

A. MicroRNAs significantly differentially expressed (FDR<0.05) between glomeruli from healthy control subjects (Control glom) and score 0, histologically normal glomeruli from FSGS patients (Glom 0). **B.** Glomerular microRNAs significantly differentially expressed (FDR<0.05) between score 2 (Glom 2) and score 0 (Glom 0) in FSGS patients. **C.** Glomerular microRNAs significantly differentially expressed (FDR<0.05) between score 2 (Glom 2) and score 1 (Glom 1) in FSGS patients. **D.** Clustered heatmap of all microRNAs significantly differentially expressed in at least one comparison between glomerular samples shown in panels A-C. **E.** Average $\log_2$ fold change relative to healthy controls for each cluster of microRNAs shown in panel D. Dashed lines indicate first and third quartiles of each cluster. Color of lines corresponds to the brackets shown in panel D. n=9 for healthy controls, 31 for FSGS score 0, 21 for FSGS score 1, and 16 for FSGS score 2.

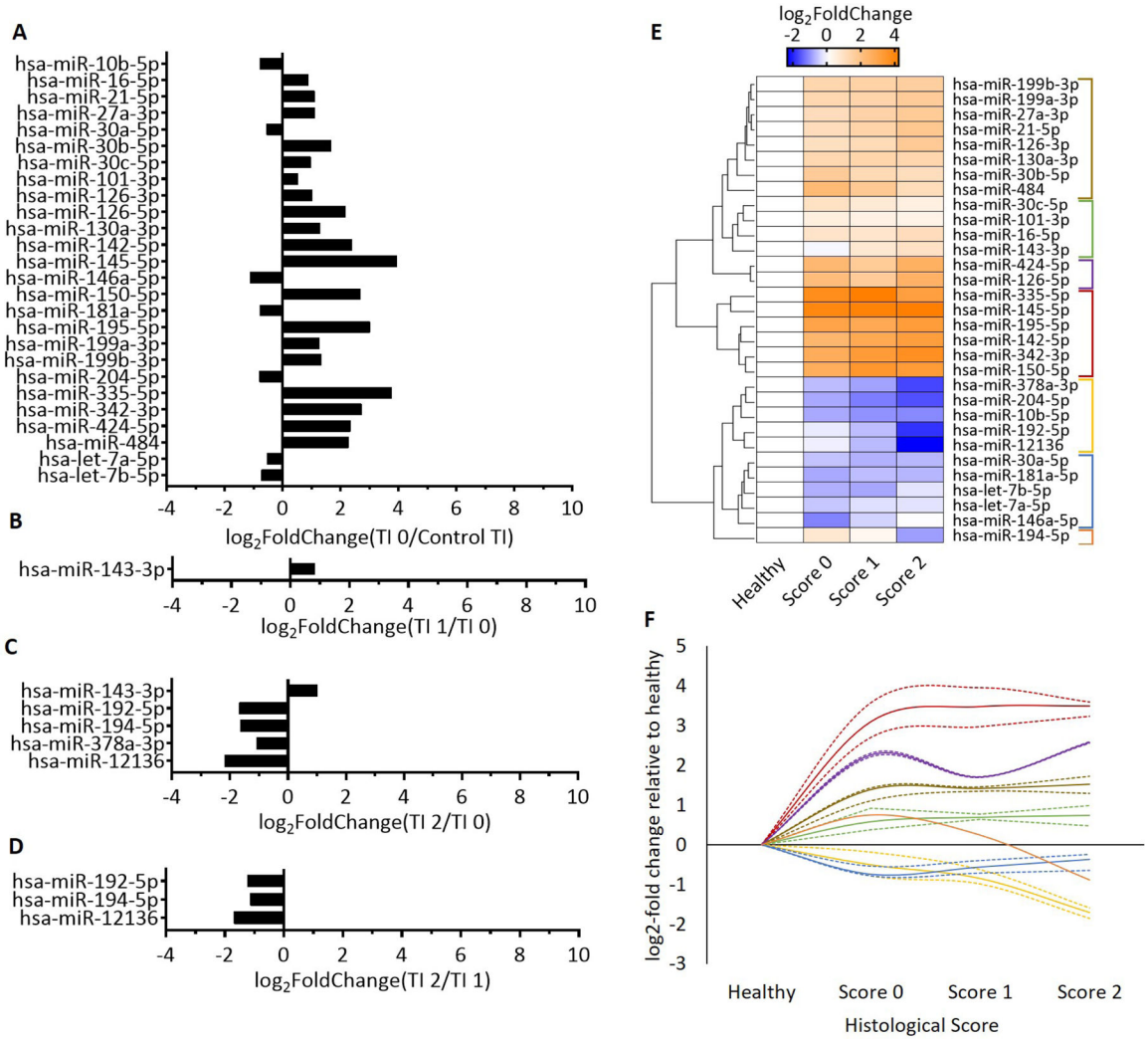

Figure 3. Tubulointerstitial microRNAs show progressive changes in expression as FSGS develops and histological injury advances.

A. MicroRNAs significantly differentially expressed (FDR<0.05) between tubulointerstitial (TI) regions from healthy control subjects (Control TI) and score 0, histologically normal TI regions from FSGS patients (TI 0). **B.** TI microRNAs significantly differentially expressed (FDR<0.05) between score 1 (TI 1) and score 0 (TI 0) in FSGS patients. **C.** TI microRNAs significantly differentially expressed (FDR<0.05) between score 2 (TI 2) and score 0 (TI 0) in FSGS patients. **D.** TI microRNAs significantly differentially expressed (FDR<0.05) between score 2 (TI 2) and score 1 (TI 1) in FSGS patients. **E.** Clustered heatmap of all microRNAs significantly differentially expressed in at least one comparison between TI samples shown in panels A-D. **E.** Average $\log_2$ fold change relative to healthy controls for each cluster of microRNAs shown in panel D. Dashed lines indicate first and third quartiles of each cluster. Color of lines corresponds to the brackets shown in panel D. n=10 for healthy controls, 13 for FSGS score 0, 26 for FSGS score 1, and 19 for FSGS score 2.

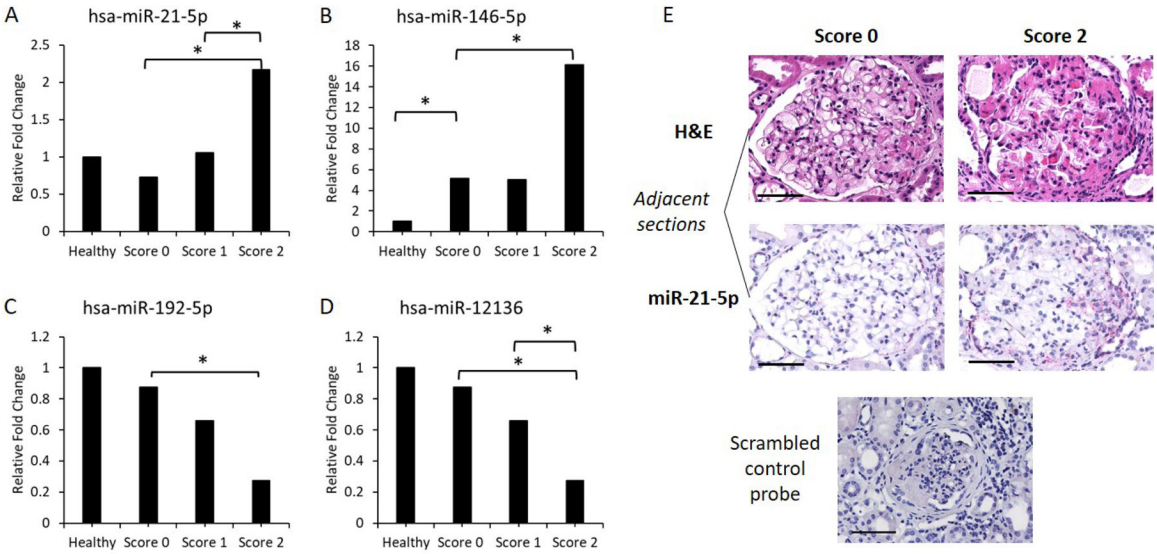

Figure 4. Representative microRNAs show progressive changes in expression as FSGS develops or histological injury advances.

A. miR-21–5p in glomeruli. **B.** miR-146b-5p in glomeruli. **C.** miR-192–5p in tubulointerstitial regions. **D.** miR-12136 in tubulointerstitial regions. Fold changes in FSGS tissue regions with score 0, 1, or 2, relative to healthy control subjects (Healthy), are shown. * indicates significant differential expression based on small RNA deep sequencing analysis (FDR<0.05). See Figures 2 and 3 for n values. E. miRNAScope analysis of miR-21–5p. Red punctate signals in the middle row of images represent miR-21–5p detection. The score 0 and score 2 glomeruli were from the same biopsy section. H&E and miR-21–5p images were taken from adjacent sections of the biopsy specimen and were representative of three score 0 glomeruli and two score 2 glomeruli found in two patients analyzed. Scale bar, 100 μm.

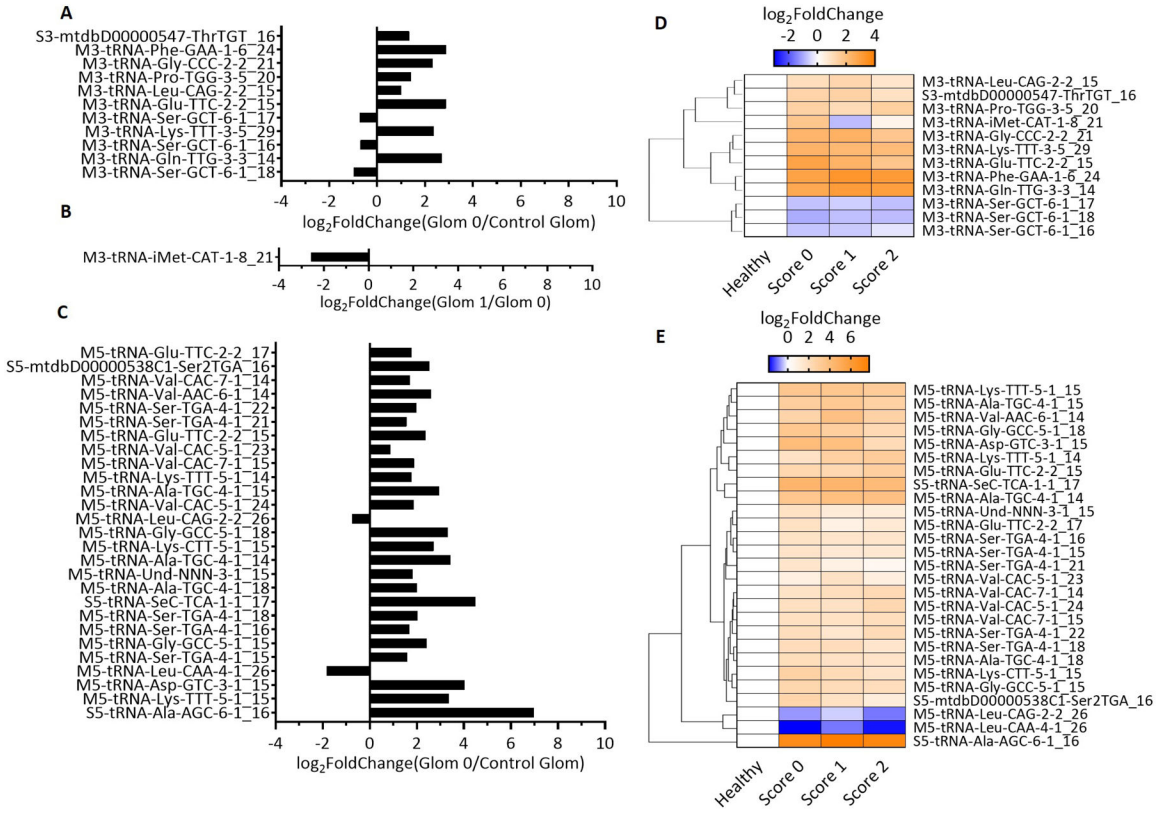

Figure 5. Glomerular tRFs are differentially expressed mainly between FSGS score 0 and healthy controls.

A. 3’-tRFs significantly differentially expressed (FDR<0.05) between glomeruli from healthy control subjects (Control glom) and score 0, histologically normal glomeruli from FSGS patients (Glom 0). **B.** A glomerular 3’-tRF significantly differentially expressed (FDR<0.05) between score 1 (Glom 1) and score 0 (Glom 0) in FSGS patients. **C.** Glomerular 5’-tRFs significantly differentially expressed (FDR<0.05) between healthy control subjects (Control glom) and score 0 from FSGS patients (Glom 0). **D.** Clustered heatmap of all 3’-tRFs significantly differentially expressed in at least one comparison between glomerular samples shown in panels A and B. **E.** Clustered heatmap of all 5’-tRFs shown in panel C. n=9 for healthy controls, 31 for FSGS score 0, 21 for FSGS score 1, and 16 for FSGS score 2.

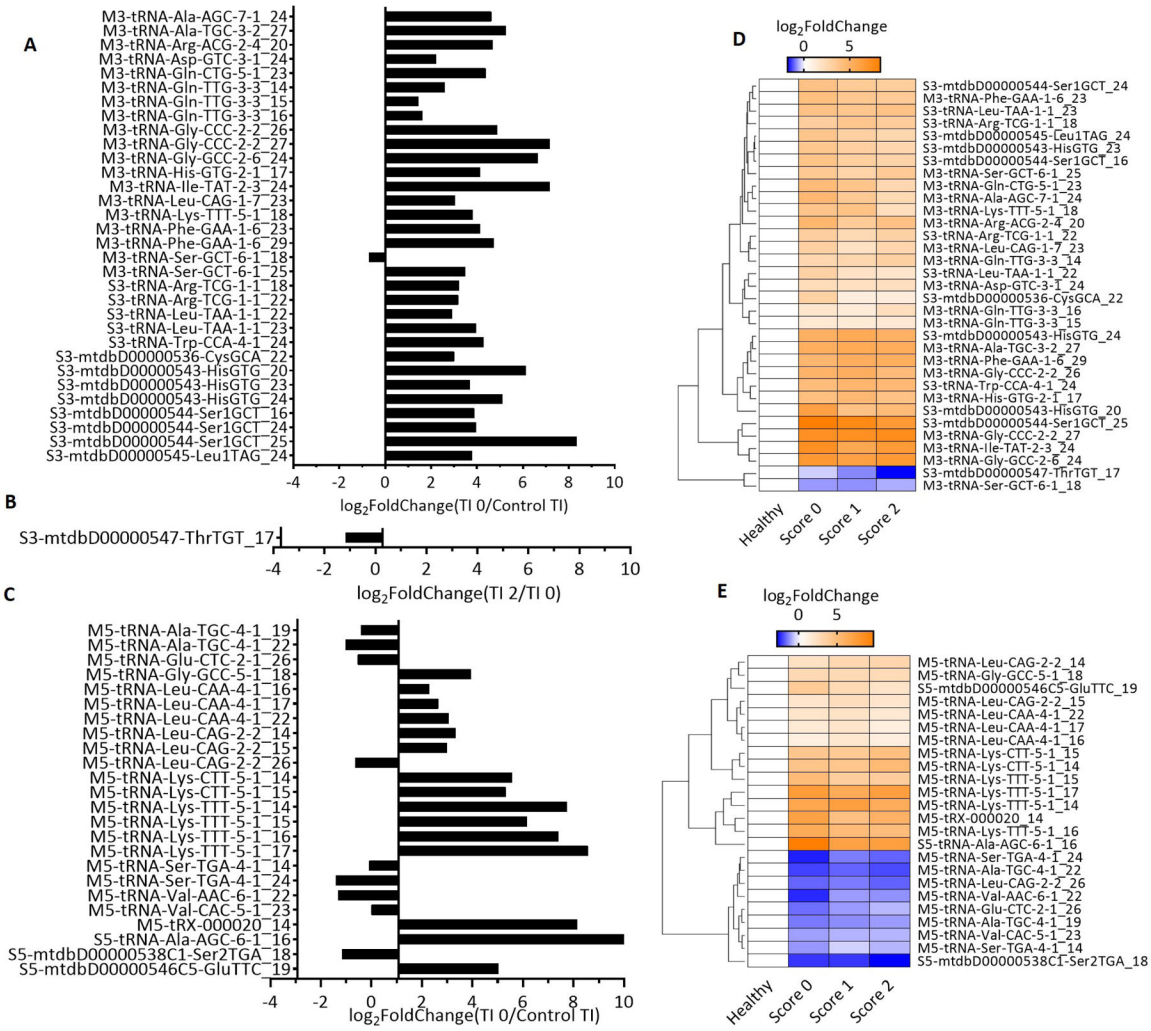

Figure 6. Tubulointerstitial tRFs are differentially expressed mainly between FSGS score 0 and healthy controls.

A. 3’-tRFs significantly differentially expressed (FDR<0.05) between tubulointerstitial (TI) regions from healthy control subjects (Control TI) and score 0, histologically normal TI regions from FSGS patients (TI 0). **B.** A TI 3’-tRF significantly differentially expressed (FDR<0.05) between score 2 (TI 2) and score 0 (TI 0) in FSGS patients. **C.** TI 5’-tRFs significantly differentially expressed (FDR<0.05) between healthy control subjects (Control TI) and score 0 from FSGS patients (TI 0). **D.** Clustered heatmap of all 3’-tRFs significantly differentially expressed in at least one comparison between TI samples shown in panels A and B. **E.** Clustered heatmap of all 5’-tRFs shown in panel C. n=10 for healthy controls, 13 for FSGS score 0, 26 for FSGS score 1, and 19 for FSGS score 2.

A

Terms Representating Pathway Clusters	healthy vs. 0	0 vs. 1 vs. 2
hsa05200: Pathways in cancer		
GO:0045596: Negative regulation of cell differentiation		
ko05206: MicroRNAs in cancer		
GO:0070848: Response to growth factor		
GO:0048732: Gland development		
R-HSA-449147: Signaling by interleukins		
GO:2000147: Positive regulation of cell motility		
GO:0048598: Embryonic morphogenesis		
GO:0010942: Postive regulation of cell death		
GO:0007507: Heart development		
R-HSA-5663202: Diseases of signal transduction by ...		
GO:0048729: Tissue morphogenesis		
GO:0097190: Apoptotic signaling pathway		
GO:0030155: Regulation of cell adhesion		
GO:1901652: Response to peptides		
GO:0080135: Regulation of cellular response to stress		
GO:0048608: Reproductive structure development		
GO:0009611: Response to woudning		
GO:0051347: Positive regulation of transferase activity		
hsa05166: Human T-cell leukemia virus 1 infection		
GO:0001568: Blood vessel development		
GO:0043408: Regulation of MAPK cascade		
R-HSA-9006934: Signaling by receptor tyrosine kinases		
GO:0070482: Response to oxygen levels		
GO:1901699: Cellular response to nitrogen compound		
GO:0070997: Neuron death		

B

Terms Representating Pathway Clusters	healthy vs. 0	0 vs. 1 vs. 2
ko05205: Proteoglycans in cancer		
ko05206: MicroRNAs in cancer		
GO:0048729: Tissue morphogenesis		
R-HSA-449147: Signaling by interleukins		
GO:0048732: Gland development		
GO:0001568: Blood vessel development		
GO:0045596: Negative regulation of cell differentiation		
GO:0030155: Regulation of cell adhesion		
GO:0048608: Reproductive structure development		
GO:0070848: Response to growth factor		
GO:0048598: Embryonic development		
GO:0010942: Positive regulation of cell death		
R-HSA-9006934: Signaling by receptro tyrosine kinases		
GO:0097190: Apoptotic signaling pathway		
GO:0070482: Response to oxygen levels		
R-HSA-5663202: Diseases of signal transduction by ...		
GO:0007507: Heart development		
GO:0043408: Regulation of MAPK cascade		
GO:0070997: Neuron death		
GO:0071396: Cellular response to lipid		
hsa01522: Endocrine resistance		
GO:0030198: Extracellular matrix organization		
GO:0009611: Response to wounding		
hsa05222: Small cell lung cancer		
GO:0001503: Ossification		
GO:0036293: Response to decreased oxygen levels		
GO:0007160: Cell-matrix adhesion		
GP:0061061: Muscle structure development		
M160: PID AVB3 integrin pathway		

Figure 7. MicroRNAs differentially expressed in histologically normal tissues in FSGS patients compared to healthy controls and as histological injury progresses in FSGS target shared but also different pathways.

A. Glomerular microRNA target pathways. **B.** Tubulointerstitial microRNA target pathways. Experimentally supported target genes for microRNAs differentially expressed in each tissue type between healthy controls and histologically normal tissue regions in FSGS (healthy vs. 0) or between FSGS tissue regions with any different histological scores (0 vs. 1 vs. 2) were retrieved and pathway enrichment analysis performed as described in Methods.

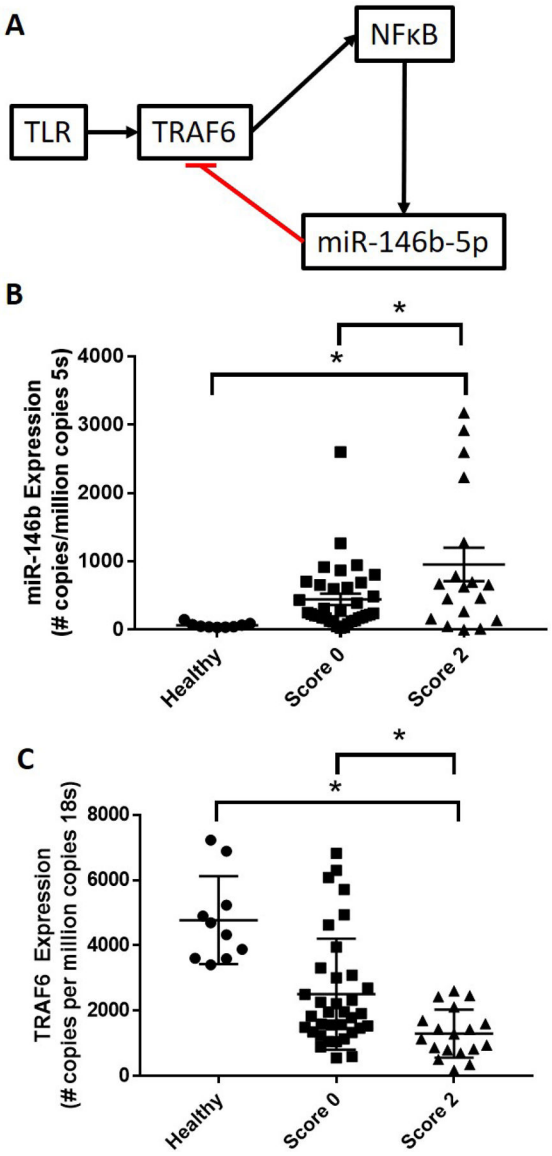

Figure 8. miR-146b-5p is progressively upregulated, and its target gene TRAF6 progressively down-regulated, in glomeruli as FSGS develops and histological injury advances.

A. Regulatory relation between miR-146b-5p and TRAF6. TLR, toll-like receptor; TRAF6, tumor necrosis factor receptor-associated factor 6; NFκB, nuclear factor kappa-light-chain-enhancer of activated B cells. **B.** miR-146b-5p abundance in glomeruli assessed by qPCR. **C.** TRAF6 abundance in glomeruli assessed by qPCR. N = 10 healthy controls, 35 score 0 (histologically normal glomeruli in FSGS patients), and 18 score 2. *, $p<0.05$ vs. healthy, one-way ANOVA followed by Holm-Sidak test.

Table 1:

Demographic and clinical information for the healthy controls and FSGS subjects.

	Healthy Controls	FSGS	p value
# of subjects	10	38	
Age at biopsy	39.2±3.9	42.8±2.4	0.82
Gender	8 M, 2 F	31 M, 7 F	0.72
Race	5 African American 3 Caucasian 2 Other	21 African American 15 Caucasian 2 Other	0.35
SBP (mmHg)	126.3±6.0	138.4±2.5	0.17
DBP (mmHg)	83.0±5.1	83.2±1.9	0.07
Serum creatinine (mg/dl)	0.96±0.04	2.49±0.26	**0.01**
eGFR (ml/min/1.73m ^{2})	>60	46.5±4.7	**0.002**
BUN (mg/dl)	11.0±1.3	32.3±3.1	**<0.001**

SBP, systolic blood pressure; DBP, diastolic blood pressure; eGFR, estimated glomerular filtration rate; BUN, blood urea nitrogen. Age differences were evaluated with Mann-Whitney Rank Sum test, gender and race evaluated with Fischer's Exact test, and SBP, DBP, serum creatinine, eGFR, and BUN evaluated with Student's t-test.